



## OPEN ACCESS

## EDITED BY

Kawaljit Kaur,  
ImmuneLink LLC, United States

## REVIEWED BY

Rui Yang,  
Shangdong Xuanzhubio, China  
Shivangi Modi,  
Prime Medicine, United States

## \*CORRESPONDENCE

Guranda Chitadze  
✉ Guranda.chitadze@uksh.de

RECEIVED 04 November 2025

REVISED 08 January 2026

ACCEPTED 12 January 2026

PUBLISHED 06 February 2026

## CITATION

Kelm M, Nasr N, Bendig S, Kabelitz D, Lustig M, Trautmann H, Laqua A, Peters C, Wesch D, Oberg H-H, Janssen O, Valerius T, Baldus CD, Scheffold A, Brüggemann M and Chitadze G (2026) Blinatumomab-driven T-cell activation in  $\alpha\beta$  and  $\gamma\delta$  T-cell subsets: insights from *in vitro* assays. *Front. Immunol.* 17:1739493. doi: 10.3389/fimmu.2026.1739493

## COPYRIGHT

© 2026 Kelm, Nasr, Bendig, Kabelitz, Lustig, Trautmann, Laqua, Peters, Wesch, Oberg, Janssen, Valerius, Baldus, Scheffold, Brüggemann and Chitadze. This is an open-access article distributed under the terms of the [Creative Commons Attribution License \(CC BY\)](https://creativecommons.org/licenses/by/4.0/). The use, distribution or reproduction in other forums is permitted, provided the original author(s) and the copyright owner(s) are credited and that the original publication in this journal is cited, in accordance with accepted academic practice. No use, distribution or reproduction is permitted which does not comply with these terms.

# Blinatumomab-driven T-cell activation in $\alpha\beta$ and $\gamma\delta$ T-cell subsets: insights from *in vitro* assays

Miriam Kelm<sup>1</sup>, Nourhan Nasr<sup>2</sup>, Sonja Bendig<sup>1,3,4</sup>, Dieter Kabelitz<sup>2</sup>, Marta Lustig<sup>3,4,5</sup>, Heiko Trautmann<sup>1</sup>, Anna Laqua<sup>1</sup>, Christian Peters<sup>2</sup>, Daniela Wesch<sup>2</sup>, Hans-Heinrich Oberg<sup>2</sup>, Ottmar Janssen<sup>2</sup>, Thomas Valerius<sup>3,4,5</sup>, Claudia Dorothea Baldus<sup>1,3,4</sup>, Alexander Scheffold<sup>2,3,6</sup>, Monika Brüggemann<sup>1,3,4</sup> and Guranda Chitadze<sup>1,3,4\*</sup>

<sup>1</sup>Medical Department II, Hematology and Oncology, Christian-Albrechts University of Kiel and University Hospital Schleswig-Holstein, Kiel, Germany, <sup>2</sup>Institute of Immunology, Christian-Albrechts University of Kiel and University Hospital Schleswig-Holstein, Kiel, Germany, <sup>3</sup>Clinical Research Unit Towards a Cure for Adults and Children with Acute Lymphoblastic Leukemia (CATCH ALL) (KFO 5010), Funded by the Deutsche Forschungsgemeinschaft (DFG, German Research Foundation), Kiel, Germany, <sup>4</sup>University Cancer Center Schleswig-Holstein (UCCSH), University Hospital Schleswig-Holstein, Kiel, Germany, <sup>5</sup>Medical Department II, Division of Stem Cell Transplantation and Cellular Immunotherapies, University Hospital Schleswig-Holstein and Christian-Albrechts-University of Kiel, Kiel, Germany, <sup>6</sup>Technische Universität Berlin, Institute for Biotechnology, Berlin, Germany

**Introduction:** Blinatumomab (BLN) is a bispecific T-cell engager that has revolutionized the treatment of B-cell precursor acute lymphoblastic leukemia (BCP-ALL), significantly improving outcomes in both adults and children. By simultaneously binding to CD19 on B cells and CD3 on T cells, BLN triggers target cell-dependent T-cell activation, resulting in the cytotoxicity of CD19<sup>+</sup> BCP-ALL cells. Despite the remarkable clinical advancements achieved with BLN, the immunological mechanisms underlying treatment response or failure remain poorly characterized.  $\gamma\delta$  T cells are attractive candidates for adoptive T-cell therapy due to potent cytotoxicity, capacity to present antigens, broad lysis of different tumor entities, and low alloreactivity. Because  $\gamma\delta$  T cells can also be redirected by BLN, we systematically studied BLN-driven effector functions *in vitro* in conventional  $\alpha\beta$  and unconventional  $\gamma\delta$  T cells from healthy donors.

**Materials and methods:** We evaluated cytotoxicity and cytokine/effector release in freshly isolated and *in vitro*-expanded  $\alpha\beta$  and  $\gamma\delta$  T cells from healthy adults against CD19<sup>+</sup> BCP-ALL cell lines (NALM-6, HAL-01), and profiled dynamic phenotypic alterations by multiparametric flow cytometry.

**Results:** CD19<sup>+</sup> targets were consistently reduced in the presence of BLN. Freshly isolated  $\alpha\beta$ , especially CD8<sup>+</sup>, displayed superior BLN-mediated effector functions as compared to  $\gamma\delta$  T cells, with donor-dependent variability in  $\gamma\delta$  killing. Notably, zoledronate-expanded V $\gamma$ 9V $\delta$ 2  $\gamma\delta$  T-cell lines achieved cytotoxicity comparable to PHA-expanded  $\alpha\beta$  cells. However,  $\gamma\delta$  T-cell-killing benefited from higher BLN concentration when challenged with high tumor load. In these *in vitro* healthy-donor T-cell cultures, BLN induced CD3 down-modulation in  $\alpha\beta$  T cells but not in  $\gamma\delta$  T cells, and  $\alpha\beta$  cultures released higher soluble Fas ligand, findings consistent with stronger early activation and suggestive of increased susceptibility to activation-associated apoptosis/AICD. Exploratory targeted single-cell transcriptomics (one donor) supported a pronounced activation/exhaustion program in  $\alpha\beta$  T cells and a

comparatively stable effector-memory profile with low checkpoint expression in  $\gamma\delta$  T cells.

**Discussion:** Together, these *in vitro* data reveal subset-specific BLN responses and support the hypothesis that *ex vivo*-expanded V $\gamma$ 9V $\delta$ 2  $\gamma\delta$  T cells could complement BLN-mediated cytotoxicity, particularly under conditions of higher CD19 density and lower target burden. These findings provide a mechanistic framework for future testing of  $\gamma\delta$  T-cell/BLN combination strategies in patient-derived models and clinical studies.

#### KEYWORDS

adoptive T-cell therapy, BCP ALL, bispecific antibody, blinatumomab, immunotherapy,  $\gamma\delta$  T cells, Zoledronate

## Introduction

The outcome of B-cell precursor acute lymphoblastic leukemia (BCP-ALL) has improved significantly over the last decade due to personalized therapy protocols and novel therapeutic strategies, including mono- or bispecific antibodies, antibody-drug conjugates, and genetically modified CAR T cells (1, 2). Nevertheless, relapse remains common, and more than 20% of patients still succumb to the disease. Outcomes are notably poorer in adults than in children, with five-year overall survival rates of around 90% in pediatric cohorts but only 40-60% in adults (3-6). This highlights the critical need to understand the mechanisms underlying therapy failure and to further optimize clinical outcomes.

Blinatumomab (BLN), a bispecific T-cell engager linking CD3 on T cells with CD19 on B cells, facilitates the formation of immunological synapses, leading to T-cell activation, expansion, and targeted lysis of CD19<sup>+</sup> cells (2, 7). Since its initial FDA approval in 2017 for relapsed or refractory B-cell precursor ALL (R/R BCP-ALL) in both adults and children, BLN has demonstrated remarkable clinical efficacy (8-11). Nonetheless, many patients relapse or fail to achieve long-term remission after BLN therapy in R/R or frontline in minimal residual disease (MRD) settings (9, 12, 13). Approximately 25% of these failures are due to loss of target antigen; the rest of the relapse cases however are due to impaired T-cell functionality (14). In heavily pretreated patients, such dysfunction may arise from prior chemotherapy regimens (15), from high leukemic burden (8, 13) or from persistent T-cell stimulation due to BLN's administration as a 28-day continuous infusion, required due to its short half-life (16, 17).

Given these limitations, exploring novel strategies to enhance BLN-mediated cytotoxicity through complementary therapeutic approaches is essential. One promising approach involves the transfer of  $\gamma\delta$  T cells from unrelated donors, a minor yet highly potent subset of T cells characterized by CD3-associated TCR  $\gamma\delta$  expression and intrinsic anti-tumor cytotoxicity irrespective of HLA-matching (18-20). Adoptive  $\gamma\delta$  T-cell therapy is attractive because  $\gamma\delta$  T cells recognize tumor cells through stress-induced

ligands without relying on HLA presentation.  $\gamma\delta$  T cells have a reduced risk of graft-versus-host disease (GvHD) and are suitable for allogeneic application across diverse patient populations (21-23).

Peripheral  $\gamma\delta$  T cells constitute up to 5-10% of circulating T cells, predominantly represented by the V $\gamma$ 9V $\delta$ 2  $\gamma\delta$  T-cell subset (18, 24, 25). These cells respond robustly to pyrophosphates ("phosphoantigens") frequently accumulating in tumor cells, and their selective activation and expansion can be reliably induced using zoledronic acid (Zole) or synthetic phosphoantigens, thus facilitating clinical-grade *ex vivo* expansion (26, 27).  $\gamma\delta$  T-cell activation depends on interactions with BTN3A1 and BTN2A1 (28, 29). Additionally,  $\gamma\delta$  T cells can function as antigen-presenting cells, cross-presenting antigens to  $\alpha\beta$  T cells and further enhancing immune responses (30, 31). Their broad tumor-recognition capacity, combined with independence of HLA-restriction, positions  $\gamma\delta$  T cells as highly favorable candidates for adoptive cell therapies across diverse malignancies, as currently explored in numerous clinical studies utilizing expanded V $\delta$ 1 and V $\delta$ 2 T-cell subsets (19). Clinical safety of allogeneic V $\gamma$ 9V $\delta$ 2  $\gamma\delta$  T-cell immunotherapy has already been documented, with prolonged survival reported in patients with late-stage lung or liver cancer (32).

Our own results suggest prognostic value of  $\gamma\delta$  T cells in ALL, with increased levels correlating to improved MRD responses post-chemotherapy (33). Limited preclinical evidence, supports the therapeutic potential of combining adoptively transferred  $\gamma\delta$  T cells with CD3-engaging antibodies, including BLN (34). However, their ability to augment BLN-mediated cytotoxicity in adoptive immunotherapy settings has not been fully evaluated. Moreover,  $\gamma\delta$  T cells may follow distinct exhaustion pathways compared to  $\alpha\beta$  T cells (35, 36), but this has not been investigated in the context of BLN.

In this *in vitro* study, we systematically investigated BLN-mediated changes in the effector functions of *ex vivo* expanded healthy donor-derived  $\gamma\delta$  T cells compared to  $\alpha\beta$  T cells. We assessed their phenotypic and functional fitness under conditions

mimicking variable tumor burdens typically encountered at diagnosis or during therapy. Our approach combined functional assays, multiparametric phenotyping, and single-cell transcriptomics to dissect how  $\gamma\delta$  T cells kill CD19<sup>+</sup> targets in the presence of BLN. A deeper understanding of these mechanisms may inform novel therapeutic strategies to improve outcomes of BLN-treated patients with BCP-ALL.

## Materials and methods

### Cell cultures

Peripheral blood mononuclear cells (PBMCs) were isolated from leukocyte concentrates of healthy adult blood donors obtained from the Institute of Transfusion Medicine (Institute for Transfusion Medicine, University Hospital Schleswig-Holstein Campus Kiel) using Ficoll density gradient centrifugation (Merck, Darmstadt, Germany). Ethical approval was granted by the institutional ethics review board of the University Medical Faculty Kiel (approval number D405/10, D479/18, D546/16). The research was conducted in accordance with the Declaration of Helsinki. CD4<sup>+</sup>, CD8<sup>+</sup>, and  $\gamma\delta$  T cells or when required entire CD3<sup>+</sup> T cells were purified from PBMCs by magnetic-activated cell sorting (MACS) using respective negative selection kits according to the manufacturer's instructions (Miltenyi Biotec, Bergisch Gladbach, Germany).

To establish  $\alpha\beta$  T-cell lines, PBMCs were stimulated with Phytohemagglutinin A (PHA; 0.5  $\mu$ g/ml; Thermo Fisher Scientific, Waltham, MA, USA) and recombinant interleukin-2 (rIL-2; 100 U/ml; Novartis, Basel, Switzerland) in culture medium which consists RPMI 1640 medium (Thermo Fisher Scientific) supplemented with penicillin (100 U/ml), streptomycin (100  $\mu$ g/ml), and 10% heat-inactivated fetal bovine serum (FBS; Thermo Fisher Scientific), hereafter referred to as culture medium, following previously established protocols (37, 38). V $\delta$ 2 T cells were expanded using Zoledronate (Zole, 2.5  $\mu$ M; Novartis) and rIL-2 (50 IU/ml) to establish short-term activated V $\delta$ 2 T-cell lines as previously reported (39). IL-2 was added every 2-3 days and cultures were split after day 6 or 7. After 14 days, non-viable cells were removed via Ficoll density centrifugation when necessary. The purity of expanded cell lines was assessed at day 14 by flow cytometry.

The human B-cell precursor ALL cell lines NALM-6 and HAL-01 obtained from DSMZ and maintained in required culture medium according to manufacturer's instructions and utilized as target cells in co-culture assays.

### Co-culture experiments

Freshly isolated CD4<sup>+</sup>, CD8<sup>+</sup>, and  $\gamma\delta$  T cells were co-cultured with HAL-01 cells at an effector-to-target (E:T) ratio of 5:1, with or without BLN (20 ng/ml) for up to 7 days (40). T-cell numbers were assessed via manual counting at day 3 and day 7 and analyzed for their composition and phenotypes by flow cytometry at day 3.

Supernatants were collected at specified day 3 and day 7, stored at  $-20^{\circ}\text{C}$ , and analyzed via ELISA as described below. *In vitro* expanded PHA-activated  $\alpha\beta$  and Zole-activated  $\gamma\delta$  T cells were co-cultured with NALM-6 or HAL-01 target cells at various E:T ratios in the presence or absence of BLN (20 ng/ml or 0.5 ng/ml) for 24 hours or 3 days. PBMCs from 6 healthy donors were co-cultured for 7 days with the CD19<sup>+</sup> BCP-ALL cell line HAL-01 at different effector-to-target (E:T) ratios: 1:1 (high CD19 load), 5:1 (medium CD19 load), or without addition of exogenous target cells (low CD19 load, autologous B cells only), in the presence of in the absence of BLN (20 ng/ml). Cells were harvested and analyzed on days 0, 3, and 7 by multiparametric flow cytometry. Effector cells at fixed numbers were cultured with varying amounts of target cells through all co-culture experiments. Recombinant human IL-2 (50 IU/ml) was added to all co-cultures at baseline and replenished every 48 h (no other exogenous cytokines were used). Media volume lost to sampling was replaced with fresh complete medium containing the same IL-2 concentration.

### Multiparametric flow cytometry

Purity of PHA- and Zole- expanded  $\alpha\beta$  and  $\gamma\delta$  T-cell cultures and MACS-isolated T-cell populations were assessed by flow cytometry using anti-CD3, CD4, CD8,  $\gamma\delta$  TCR, and  $\alpha\beta$  TCR monoclonal antibodies. Only populations with >80-90% purity were used in co-culture assays. For all analyses, cells were gated on singlets and live cells defined based on scatter properties, followed by CD3<sup>+</sup> lymphocytes and subsequent  $\alpha\beta/\gamma\delta$  and memory-subset gates (Supplementary Table 1, gating strategy depicted in Supplementary Figures 1, 2).

B-cell depletion in BLN-activated PBMCs or in co-cultures was analyzed on BD FACS Canto using antibodies directed against CD19 and CD3 or at Cytex Northern Lights cytometer using a 22-color antibody panel also incorporating anti-CD3 and anti-CD19 with the following antibodies directed against CD4, CD8, CD25, CD27, CD28, CD38, CD45, CD45RA, CD56, CD95, Annexin V, CCR7, DNAM-1, HLA-DR, PD-1,  $\gamma\delta$  TCR, TIGIT, TIM-3, V $\delta$ 2  $\gamma\delta$  TCR and 7-AAD.

Selected samples undergoing single-cell RNA sequencing (BLN-treated and untreated samples of single healthy donor T cells) were analyzed using antibodies against CD3, CD4, CD8, CD16, CD19, CD22, CD24, CD45, CD45RA, CD56, CCR7, DNAM-1,  $\gamma\delta$  TCR and V $\delta$ 2  $\gamma\delta$  TCR. Samples were analyzed on a BD FACSLyric. Detailed information of used antibody panels and used clones or formats is provided in Supplementary Table 2.

### Enzyme-linked immunosorbent assay

Cell culture supernatants were analyzed for Interferon- $\gamma$  (IFN $\gamma$ ; DIF50C), Granzyme B (GrzB; DGZB00), Perforin (QK8011), Granulysin (Gnly; DY3138), Perforin (Prf; QK8011) and soluble Fas-Ligand (sFAS-L; DFL00B) using sandwich ELISA kits from R&D Systems, Minneapolis, USA according to the manufacturer's

instructions. Absorbance was measured at 450 nm using a microplate reader (Tecan Group Ltd, Männedorf, Switzerland) in the Institute of Immunology Kiel.

## Determination of CD19 antigen-density

To quantify CD19 antigen density on the cell surface of BCP ALL cell lines (NALM6 and HAL-01), the specific antibody binding capacity (SABC) was determined using the purified anti-human CD19 antibody (clone HIB19) and the QIFIKIT<sup>®</sup> (DAKO, Glostrup, DK) by flow cytometry according to the manufacturer's instructions in the Division of Stem Cell Transplantation and Cellular Immunotherapies.

## BD Rhapsody single-cell RNA-seq

BD Rhapsody Single-Cell Analysis System (BD, Biosciences) were utilized using a targeted approach with human T-cell Expression Panel commercially available from BD Biosciences and covering 259 genes, commonly expressed in human T cells (Cat ID 633751, [Supplementary Table 3](#)). For this, PBMCs from one healthy donor were cultured for 72 hours with rIL-2 (50 IU/ml) + BLN (20 ng/ml) or with rIL-2 alone as a control. Afterwards, CD3<sup>+</sup> cells were negatively isolated (human MACS Pan T-cell isolation Kit, Miltenyi Biotec), labeled using BD Single-Cell Multiplexing Kit and AbSeq (antibody-labeled with oligos) reagents targeting CD4, CD8, CD25, CD45RA, CD127, CCR7, and TCR $\gamma\delta$  ([Supplementary Table 2](#)). Cells from BLN-treated and control samples were labeled with Sample Tags following the manufacturer's instructions (Single Cell Labelling with the BD<sup>TM</sup> Single-Cell Multiplexing Kit and BD<sup>TM</sup> AbSeq Ab-Oligos (ID: 214419 Rev. 2.0)). 10, 000 single cells were load on a cartridge with preloaded beads to capture RNA of single cell, followed by cDNA synthesis using the BD Rhapsody Express Instrument and Scanner following BD protocols (Single Cell Capture and cDNA Synthesis with the BD Rhapsody<sup>TM</sup> Single-Cell Analysis System (210966 Rev. 1.0)). cDNA libraries of target transcripts, Samples Tags and Abseqs were prepared using the Manufactures instructions, following mRNA Targeted, Sample Tag, and BD<sup>TM</sup> AbSeq Library Preparation with the BD Rhapsody<sup>TM</sup> Targeted mRNA and AbSeq Amplification Kit (214508 Rev. 3). The final libraries were quantified using a Qubit Fluorometer with the Qubit dsDNA HS Kit (ThermoFisher) and the size-distribution was measured using the Agilent high sensitivity D5000 assay on a TapeStation 4200 system (Agilent Technologies). Sequencing was performed in paired-end mode (2x75 cycles) on NextSeq 500 System (Illumina) with NextSeq 500/550 Mid Output Kit, generating approximately 1.3 billion reads. Data processing utilized the Seven bridges pipeline BD Rhapsody<sup>TM</sup> Targeted Analysis Pipeline - Revision: 0. Generated demultiplexed matrices of ScrNA-seq UMI count were imported to R 4.3.3 and gene expression data analysis was performed using the R/Seurat package 5.3.0 (41). To remove doublets and cell fragments, we further fitted a linear model of detected genes versus transcript count per sample

and excluded deviating outliers (0.5 - 5% of cells, depending on sample quality). Additionally, we removed genes that were expressed in less than ten cells. Before downstream analysis, LogNormalization (Seurat function) was applied separately to the RNA and AbSeq assays. The data were then scaled regressing for total UMI counts and principal component analysis (PCA) was performed. RNA and AbSeq data were integrated using weighted nearest neighbors (WNN) based on the first 8 RNA and first 6 AbSeq principal components. UMAP and clustering were performed on the resulting WNN graph. For two-dimensional data visualization we performed UMAP based on the first 20 dimensions of the resulting WNN graph. The cells were clustered using the Louvain algorithm based on the first 20 dimensions with a resolution of 0.8. Cluster annotation was based on gene expression signatures (top 5 characteristic genes per cluster) and AbSeq expression ([Supplementary Table 4](#)).

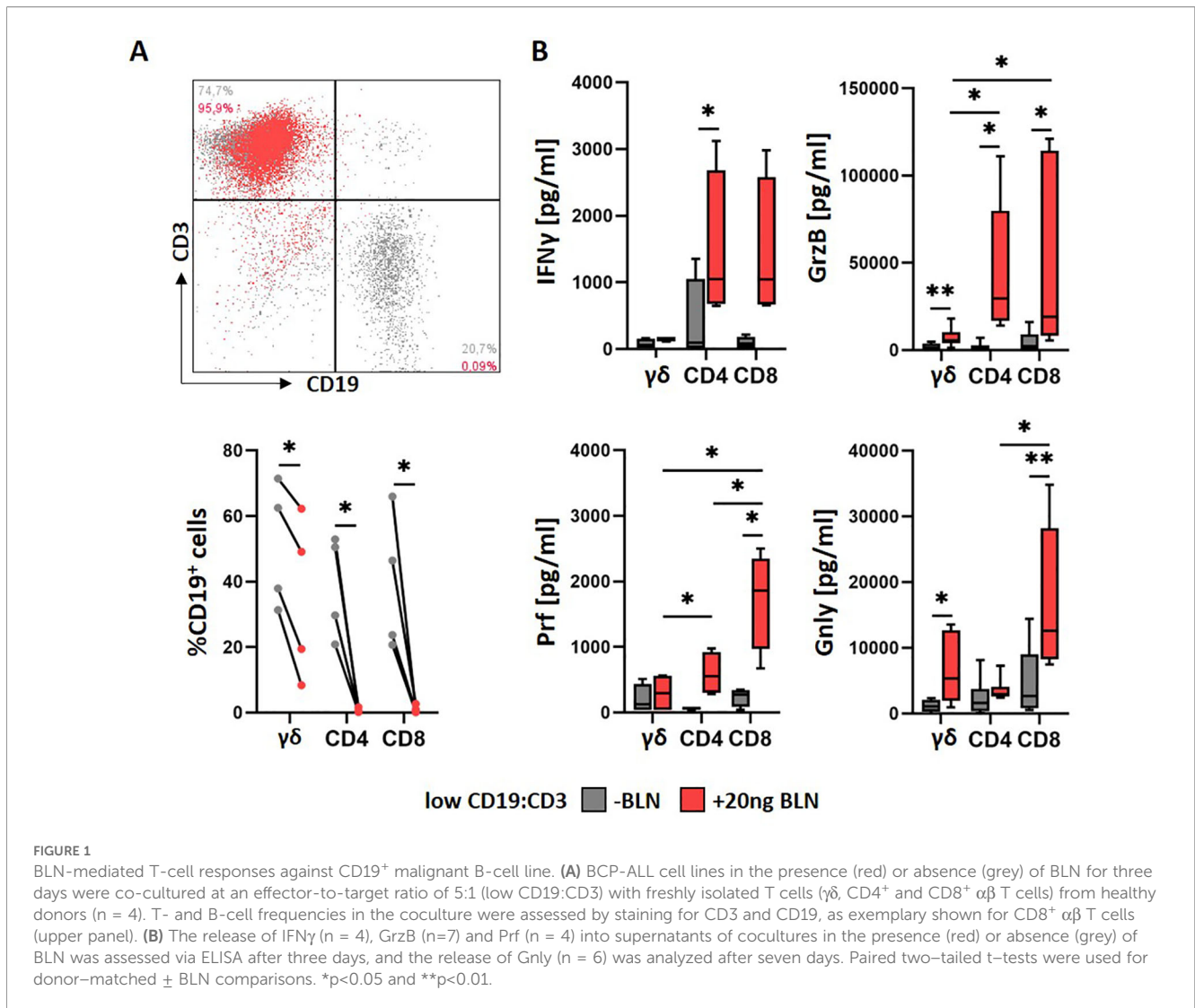
## Statistical analysis

For paired comparisons of matched donors, we used two-tailed paired t-tests. For comparisons between non-overlapping donor sets, we used two-tailed unpaired t-tests. For multiparameter immunophenotyping, p-values were adjusted for multiple testing using the Benjamini-Hochberg false discovery rate (FDR) method across the set of markers/subsets tested within each comparison. In all figures, n denotes the number of independent donors (biological replicates). No multiple-comparison adjustment was applied to ELISA readouts because each analyte was analyzed as an independent, pre-specified endpoint (single assay per analyte), whereas FDR correction was applied to high-dimensional flow-cytometry marker panels. Statistical significance was set at p<0.05 (\*), p<0.01 (\*\*), p<0.001 (\*\*\*). Analyses were performed using GraphPad Prism 8.4.3 and RStudio 4.3.3.

## Results

### BLN potentiates cytotoxicity of fresh $\alpha\beta$ and $\gamma\delta$ T cells, but $\alpha\beta$ T cells dominate early cytotoxicity

We first evaluated BLN-induced killing of CD19<sup>+</sup> target cells by freshly isolated  $\gamma\delta$ , CD4<sup>+</sup> and CD8<sup>+</sup>  $\alpha\beta$  T-cell populations. Isolated T-cell populations ( $\gamma\delta$ , CD4<sup>+</sup> and CD8<sup>+</sup>  $\alpha\beta$ ) were co-cultured with the CD19<sup>+</sup> malignant BCP ALL cell line HAL-01 at an effector-to-target ratio of 5:1 in the presence of BLN at concentration of 20 ng/ml, previously demonstrated to effectively induce immunological synapse formation (40). At day three, target CD19<sup>+</sup> cells were consistently reduced in all co-cultures in the presence of BLN, as measured by assessing residual CD19<sup>+</sup> cells using flow cytometry ([Figure 1A](#), top panel shown for CD8<sup>+</sup>  $\alpha\beta$  T cells). However,  $\gamma\delta$  T cells displayed lower cytolytic activity compared to CD8<sup>+</sup> and CD4<sup>+</sup>  $\alpha\beta$  T cells, demonstrated by persistence of CD19<sup>+</sup> target cells in  $\gamma\delta$  and not in  $\alpha\beta$  T-cell cultures in the presence of BLN ([Figure 1A](#),



bottom panel). To account for donor-dependent background killing, we additionally quantified BLN-specific target elimination by normalizing each donor to its no BLN condition (Supplementary Figure 3A): residual CD19<sup>+</sup> cells in the no BLN condition were set to 100%, and the corresponding +BLN condition was expressed relative to this baseline (i.e., a donor-normalized fold-reduction metric). This normalization did not change the overall conclusion that CD8<sup>+</sup> and CD4<sup>+</sup>  $\alpha\beta$  T cells mediated stronger BLN-dependent killing than  $\gamma\delta$  T cells.

ELISA assays revealed significantly increased secretion of Interferon- $\gamma$  (IFN $\gamma$ ) and cytotoxic effector molecule Granzyme B (GrzB), Perforin (Prf) and late mediator of cytotoxicity Granulysin (Gnl) (42). At day 3 in BLN-treated cultures, with  $\alpha\beta$  T cells releasing consistently higher levels than  $\gamma\delta$  T cells. Prf levels were highest in CD8<sup>+</sup> T-cell cultures at day 3, whereas Gnl levels, assessed after seven days, were significantly elevated in both CD8<sup>+</sup> and  $\gamma\delta$  T-cell cultures treated with BLN (Figure 1B).

Overall, BLN enhanced cytotoxic potential of freshly isolated  $\gamma\delta$  and  $\alpha\beta$  T-cell populations. However  $\alpha\beta$  T-cell populations demonstrated superior BLN-mediated cytolytic activity compared

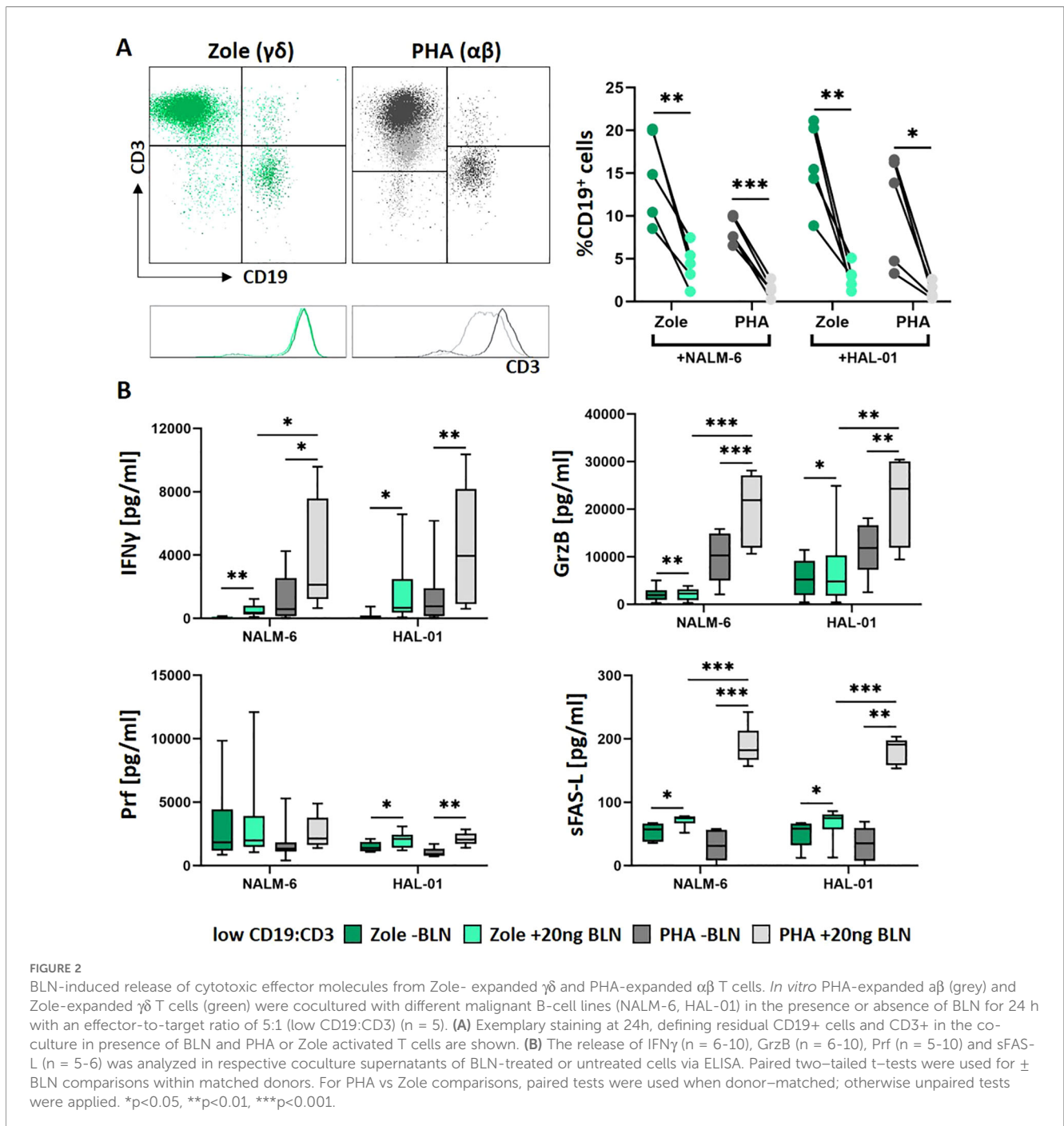
to  $\gamma\delta$  T cells, with CD8<sup>+</sup> T cells having the potentially highest cytotoxic potential, as indirectly indicated by perforin secretion (43).

## Activated $\gamma\delta$ T cells match $\alpha\beta$ cytotoxicity under favorable antigen conditions

Given the known cytotoxic potential of Zole-activated V $\delta$ 2 T cells and their potential clinical application (19, 44), we next assessed BLN-dependent killing using Zole-expanded V $\gamma$ 9V $\delta$ 2  $\gamma\delta$  T-cell lines. Using the same flow-based readout (residual CD19<sup>+</sup> cells), we compared their activity with PHA-expanded  $\alpha\beta$  T cells against HAL-01 and NALM-6, which differ in CD19 surface density (HAL-01 ca. 2.5-fold higher CD19 antigen density than NALM-6; Supplementary Figure 4). We studied release of cytokine mediators/effector molecules at 24 hours anticipating stronger effector functions (Figure 2B) in the presence of BLN by Zole-expanded  $\gamma\delta$  T cells (Figure 2A, green) and compared it with effector functions mediated by PHA-expanded  $\alpha\beta$  T cells

(Figure 2A, grey) against two BCP-ALL cell lines, HAL-01 and NALM-6, with high and low expression CD19-patterns respectively (Supplementary Figure 4). At an effector-to-target ratio of 5:1 and BLN concentration of 20 ng/ml, both  $\gamma\delta$  and  $\alpha\beta$  activated cultures resulted in significant CD19<sup>+</sup> reduction. However, PHA-expanded  $\alpha\beta$  T cells induced a slightly more pronounced B-cell killing with complete clearance of CD19<sup>+</sup> cells. Target cells still persisted in Zole-expanded  $\gamma\delta$  T cells after 24 hours at low levels, particularly in a case of NALM6 (residual CD19<sup>+</sup> cells at median value of 4.4% of co-culture), expressing lower levels of CD19 compared to HAL-01 (Supplementary Figure 4). Interestingly, we observed CD3

downregulation, that selectively occurred in PHA-expanded  $\alpha\beta$  T cells in the presence of BLN, whereas Zole-expanded  $\gamma\delta$  T cells maintained stable CD3 expression (Figure 2A, bottom panel with exemplary histograms). BLN-independent T-cell responses were also observed, as indicated by partial B-cell elimination in the absence of BLN occurring in a donor-dependent manner, with PHA-expanded  $\alpha\beta$  T cells (dark grey) outperforming Zole-expanded  $\gamma\delta$  T cells (dark green). BLN-dependent T-cell responses were also calculated by normalized residual CD19-cells to their counts in the absence of BLN and resulted in the same outcome (Supplementary Figure 3B).



Both expanded  $\gamma\delta$  and  $\alpha\beta$  T-cell lines exhibited increased secretion of IFN $\gamma$ , GrzB, soluble FAS ligand (sFAS-L), and Prf following BLN stimulation in the presence of tumor cells. IFN $\gamma$  and GrzB were lower in Zole-expanded cultures compared to PHA-expanded cultures (Figure 2B). Interestingly, high levels of sFAS-L, known to occur during activation induced cell death (AICD) expected in case of excess of T-cell activation (45, 46), was higher in the presence of PHA-expanded  $\alpha\beta$  T cells compared to Zole-expanded  $\gamma\delta$  T cells. Thus, when comparing Zole and PHA-activated T-cell cultures,  $\alpha\beta$  T-cells exhibit superior cytotoxicity; however, release higher levels of soluble FAS-L and potentially undergo CD3 downregulation in contrast to  $\gamma\delta$  T cells.

## Target antigen density/tumor burden jointly impact $\gamma\delta$ efficacy; higher BLN dose preferentially benefits $\gamma\delta$ under stress

In clinical setting, response to BLN is largely dependent on ALL blast counts (8). Blinatumomab has higher affinity to CD19 and lower affinity to CD3 (47). BLN binds to CD19 and acts as activation matrix for T cells, that can detach and kill up to 5-10 target cells within 9 hours (Serial killing) (48, 49). In the absence of CD19<sup>+</sup>, no T-cell activation takes places (47). Thus, CD19 target expression is relevant for BLN mediated T-cell activation and target antigen density/target cell load, as well as the concentration of BLN might impact T-cell signaling and activation (8). Thus, we next explored how varying the effector-to-target ratio and BLN concentration influenced  $\gamma\delta$  T-cell cytotoxicity. Using the HAL-01 cell line, which exhibits higher CD19 antigen density than NALM-6 (ca. 2.5-fold; Supplementary Figure 4), we cultured Zole-expanded  $\gamma\delta$  T-cell lines under low target burden (E:T 5:1; MRD-like) and high target burden (E:T 1:5; diagnosis/relapse-like) conditions (Figure 3). BLN was tested at 20 ng/ml and at concentration of 0.5 ng/ml, close to steady-state serum level reported in patients (50). Residual target (CD19<sup>+</sup>) cells and T-cell composition/phenotypes linked with T-cell functionality were evaluated after 24 hours and following three days by 22-color spectral flow cytometry (Supplementary Table 2).

Under low target burden (E:T 5:1; low CD19:CD3), both  $\gamma\delta$  (Zole-expanded) and  $\alpha\beta$  (PHA-expanded) cultures efficiently eliminated CD19<sup>+</sup> target cells (Figure 3A, right panel). Under high target burden (E:T 1:5; high CD19:CD3, Figure 3A, left panel),  $\alpha\beta$  T-cell cytotoxicity appeared near-maximal already at 24 h and did not increase further with higher BLN, whereas  $\gamma\delta$  T-cell killing improved with 20 ng/ml BLN, particularly by day 3 (3/5 donors; Figure 3A, left panel, green bars). BLN-specific target cell elimination based on donor-normalized residual target cells yielded the same pattern (Supplementary Figure 3C).

Consistent with previous findings, marked CD3 downregulation was observed predominantly in  $\alpha\beta$  T cells upon BLN treatment, especially at high tumor burden conditions (Figures 3B, C; Supplementary Figure 5). Because CD3 downmodulation occurred only at high target burden, and spared  $\gamma\delta$  T cells while primarily affecting  $\alpha\beta$  T cells under identical BLN and

staining conditions, this pattern is consistent with CD3 internalization after strong T-cell stimulation rather than epitope masking (51), supported by the condition-matched unstained controls and representative histograms (Supplementary Figure 5).

## Zole-expanded $\gamma\delta$ T cells retain a stable effector memory phenotype with low checkpoint expression under BLN

The differential CD3 modulation observed in  $\gamma\delta$  and  $\alpha\beta$  T cells suggested distinct BLN-mediated signaling through CD3, which we hypothesized would result in phenotypic and functional differences, affecting their fitness and potentially susceptibility to AICD, as supported by the high levels of sFAS-L detected in  $\alpha\beta$  T-cell cultures. Of note, sFas-L reflects ADAM10/17-mediated shedding of the pro-apoptotic membrane FasL and elevated sFasL in CD8<sup>+</sup> cultures are here interpreted as a biomarker of strong re-stimulation and shedding, not as a direct driver of AICD (45, 46, 52).

To investigate this, we compared the composition and phenotype of Zole- and PHA-expanded T cells from 5 healthy donors at baseline (prior to co-culture) and analyzed their numbers and phenotypic changes at day 1 and day 3 using spectral flow cytometry (Figure 4, Supplementary Figure 6). At baseline prior co-culture (d0), after 14 days of expansion, T-cell composition differed markedly: Zole-expanded cultures consisted expectedly of V $\delta$ 2  $\gamma\delta$  T cells (median 90%, range 80-97%), while PHA cultures comprised both CD4<sup>+</sup> and CD8<sup>+</sup>  $\alpha\beta$  T cells with median proportions of 14% (range 6%-31%) and 66% (range 63%-84%), respectively (Supplementary Table 1).

Zole-expanded V $\delta$ 2  $\gamma\delta$  T cells displayed a highly homogeneous effector memory (EM) phenotype (CD27<sup>+</sup>CD45RA<sup>+</sup>), consistent with previous observations (39, 44). Their absolute cell counts did not significantly change during three days of co-culture across different BLN concentrations at high ALL load (Figure 4C, left top panel, black line). We observed slight decrease in absolute counts in low CD19:CD3 conditions (Figure 4C, right top panel, black line). Day 14 Zole-expanded  $\gamma\delta$  T cells expressed high levels of activation markers (CD38, HLA-DR, DNAM-1, CD56) while showing lower or absent levels of exhaustion markers such as TIGIT (baseline, d0). During co-culture there was not significant change of their phenotype compared to baseline (Figure 4A). TIGIT negativity on day 14 cultures goes in line with a reported transient peak around day 4 and declining by day 7 in Zole-expanded T-cell cultures (35).

In contrast, PHA-expanded CD8<sup>+</sup>  $\alpha\beta$  T cells were more heterogeneous with naïve and memory subsets at baseline. Upon BLN stimulation, especially in the context of high tumor load, naïve cells declined and EM and TEMRA (CD27<sup>+</sup>CD45RA<sup>+</sup>) subsets increased after 24 hours, with EM cells becoming dominant by day 3 (Figure 4B). This was reflected by an increase in total EM counts in the presence of high tumor load at day 3 (unadjusted  $p=0.019$ ; FDR-adjusted  $p=0.09$ , trend), as single dominant population. In cultures with lower CD19<sup>+</sup> burden (Figure 4C, left bottom panel), in line with less activation provided by low target cell

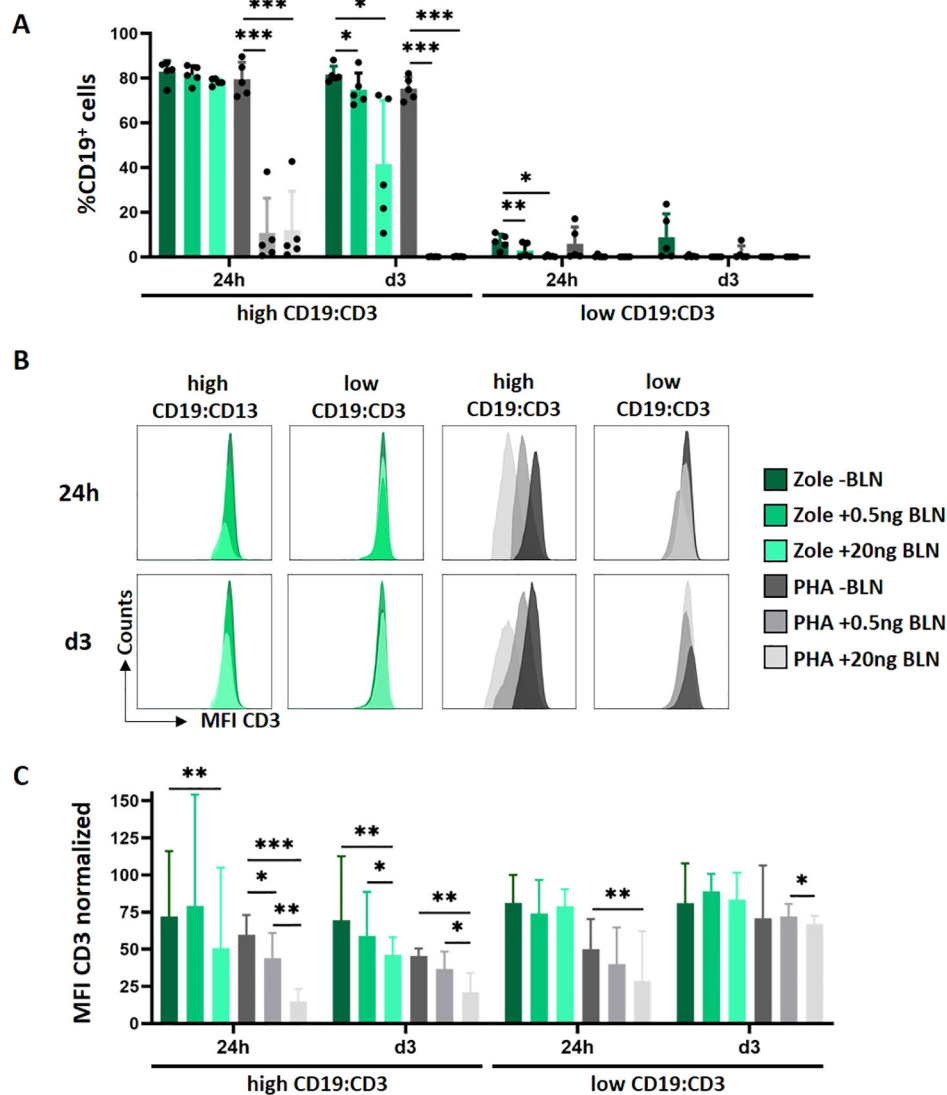


FIGURE 3

Impact of tumor burden and BLN concentration on T-cell-mediated cytotoxicity in Zole ( $\gamma\delta$ ) - and PHA ( $\alpha\beta$ )-expanded T cells. (A) Median B-cell decline of HAL-01 cells from Zole- (green) and PHA-expanded T cells (grey) healthy donors ( $n = 5$ ). Individual values are represented by dots. (B) Representative example of CD3-expression in  $\gamma\delta$  and  $\alpha\beta$  T-cell cultures, following BLN-mediated activation. (C) Normalized CD3 MFI of different culture conditions ( $n = 5$ ). High = High Tumor load (E:T 1:5), Low = Low Tumor load (ET 5:1). CD3 MFI was normalized to the corresponding unstained control (CD3 MFI/unstained MFI). Paired two-tailed t-tests were used for donor-matched  $\pm$  BLN comparisons. \* $p < 0.05$ , \*\* $p < 0.01$ , \*\*\* $p < 0.001$ .

density, naïve CD8<sup>+</sup> T cells transitioned toward both EM and central memory (CM) phenotypes. Interestingly absolute counts in the presence of low target cells and lower BLN amount was higher compared to high target density and low BLN concentration. Phenotypic shifts observed in PHA-expanded CD4<sup>+</sup>  $\alpha\beta$  T cells following BLN are shown as [Supplementary Figure 6](#).

Phenotypically, PHA-expanded CD8<sup>+</sup>  $\alpha\beta$  T cells showed strong activation in response to BLN, characterized by increased expression of CD25 and HLA-DR in line to observed differentiation from naïve to memory phenotypes. TIGIT expression was markedly high in  $\alpha\beta$  T cells at baseline. We also attempted to study differences in AICD at 24h or at day 3, however we did not observe differences in Annexin-V expression on T cells

following BLN stimulation (readout for AICD), possibly because AICD often peaks within 4-12 h of stimulation.

### BLN expands CD4<sup>+</sup> and CD8<sup>+</sup> but not $\gamma\delta$ T cells from mixed PBMC cultures

Next, we asked whether BLN treatment in a mixed PBMC context could induce  $\gamma\delta$  T-cell proliferation alongside  $\alpha\beta$  T cells, despite unfavorable abundances of  $\gamma\delta$  T cells. This particular point is important in the clinical setting. To this end we stimulated PBMCs ( $n = 6$ ) together with CD19<sup>+</sup> HAL-01, at an E:T ratio of 1:1 (corresponding more to high CD19<sup>+</sup> load when taking CD3 T-

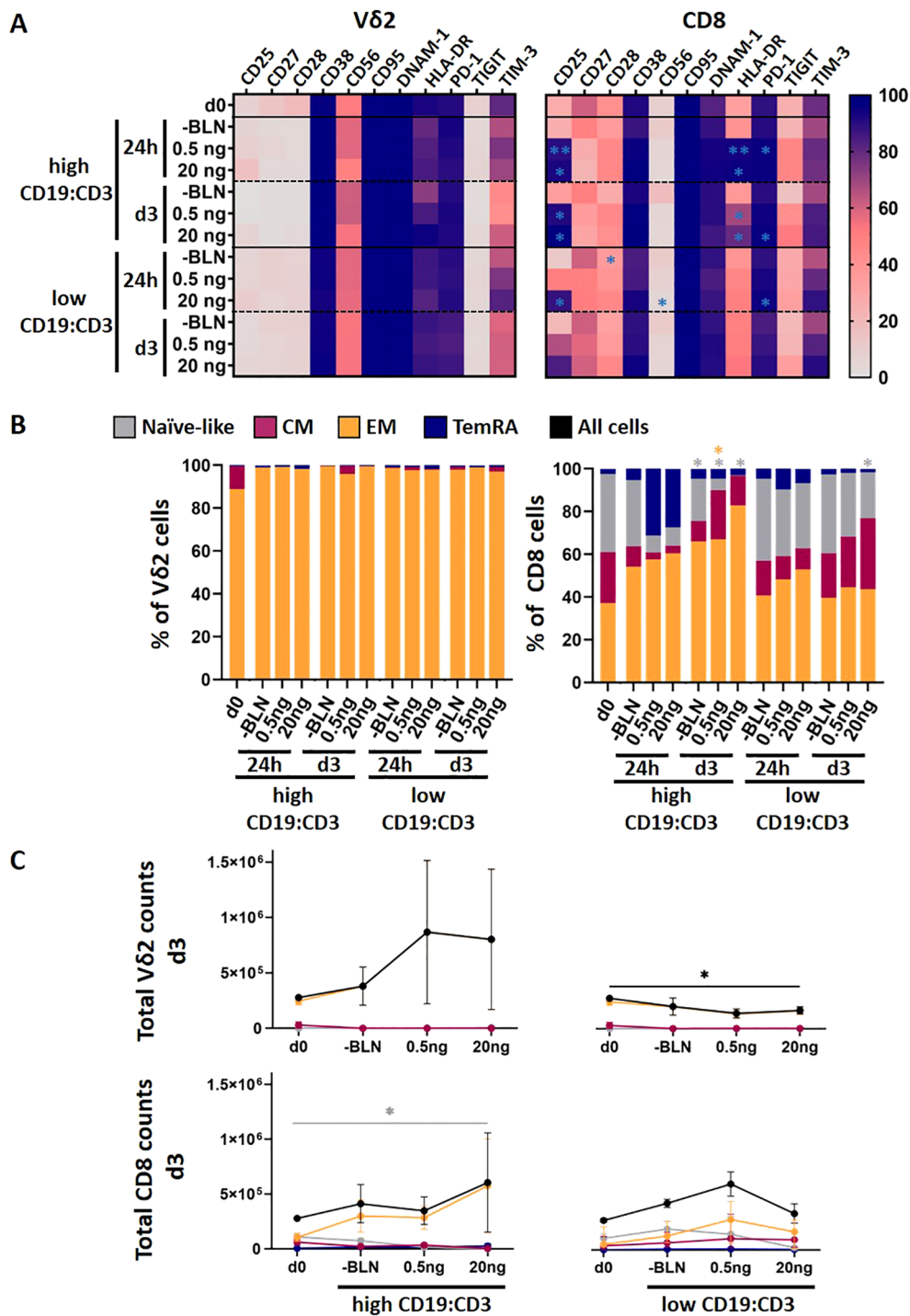
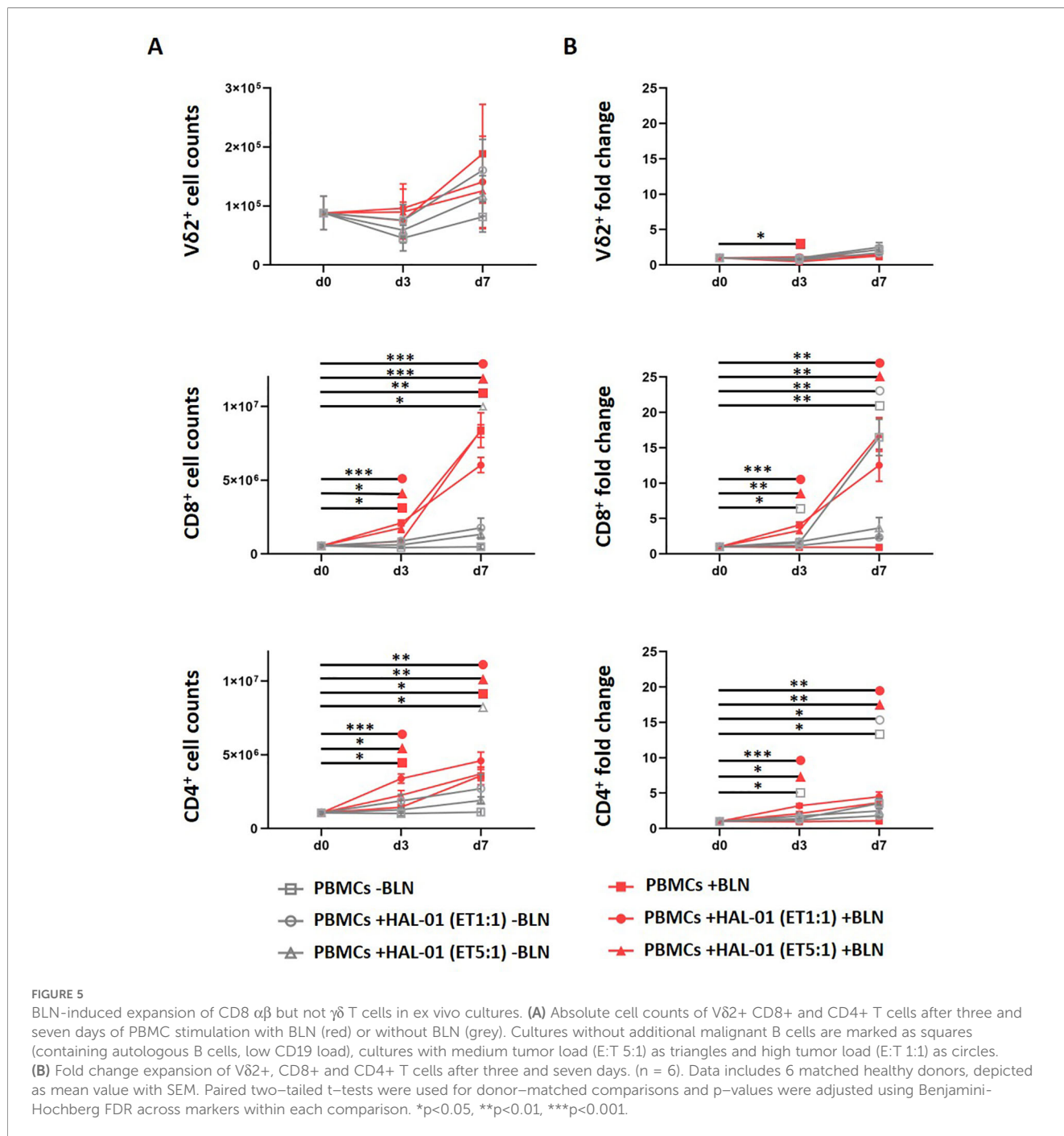


**FIGURE 4** Phenotypic differences between PHA and Zole activated  $\alpha\beta$  and  $\gamma\delta$  T cells. **(A)** Mean Marker Expression on Zole-expanded Vdelta2 and PHA-expanded CD8 T cells at baseline, at day 1 and day 3 following co-culture with high (E:T 1:5) and low tumor load (n = 5). **(B)** Mean values of EM, CM, Naïve and TEMRA cells of CD8 and Vdelta2 cells. **(C)** Absolute cell counts of EM, CM, Naïve and TEMRA cells of CD8 and Vdelta2 cells at day 0 and day 3. Data includes 5 matched healthy donors, depicted as mean value with SEM. Paired two-tailed t-tests were used for donor-matched comparisons between baseline and co-culture conditions and p-values were adjusted using Benjamini-Hochberg FDR across markers within each comparison. \*p<0.05, \*\*p<0.01, \*\*\*p<0.001.

cell proportions of PBMCs into account), at an E:T ratio of 5:1 (medium CD19<sup>+</sup> load) and without addition of CD19-expressing cell lines (low CD19<sup>+</sup> load, autologous B-cells) for 7 days with (red) and without (grey) 20 ng/ml BLN (Figure 5A). We assessed absolute

cell counts of CD4<sup>+</sup>, CD8<sup>+</sup> and  $\gamma\delta$  T cells at day 0, day 3 and day 7 of the co-culture (Supplementary Figure 7) and assessed immune profiles of T cells. We noticed a significant expansion of CD4<sup>+</sup> and CD8<sup>+</sup> T cells in all three culture conditions with BLN treatment



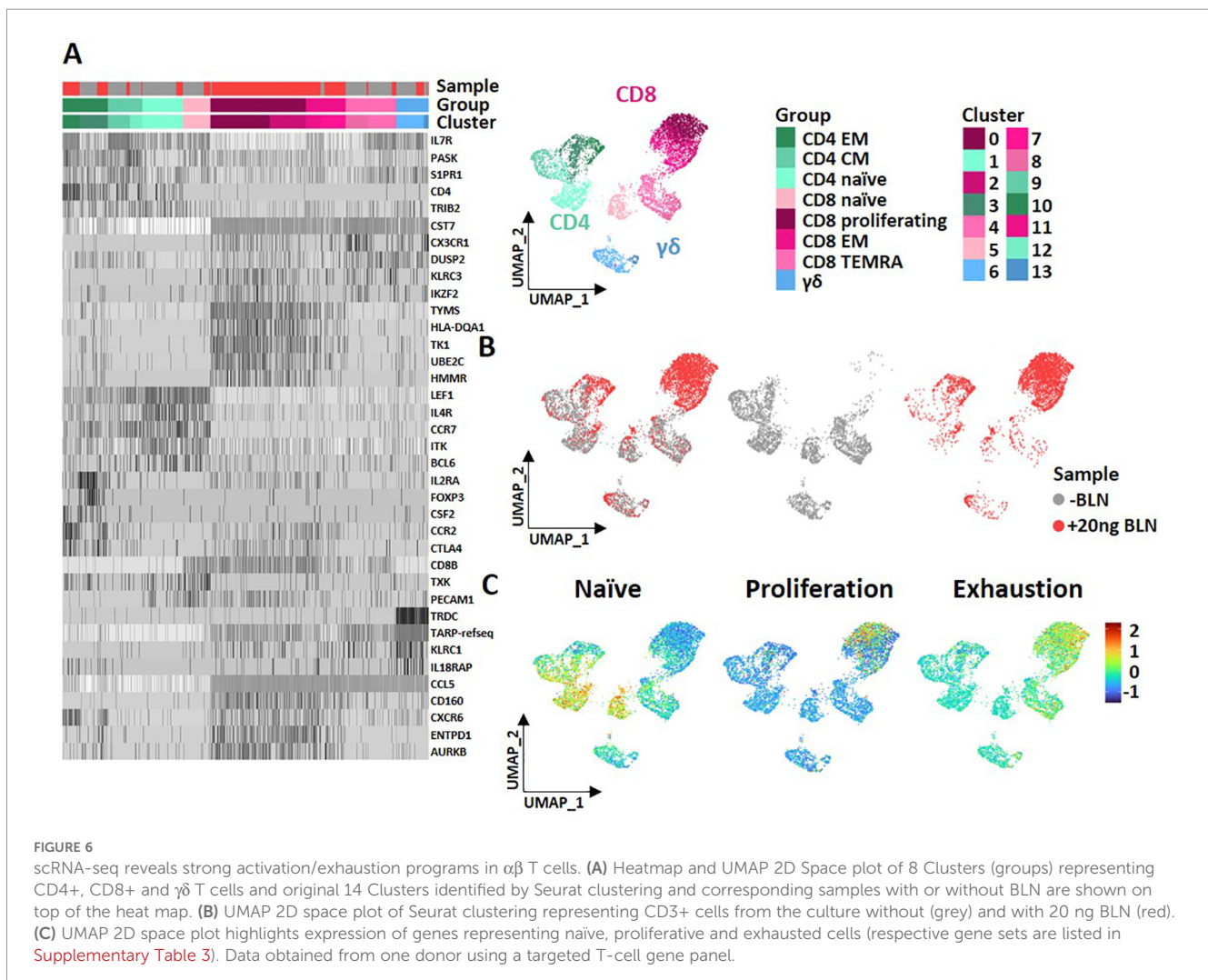
with low, medium and high CD19<sup>+</sup> load. In contrast to CD4<sup>+</sup> and CD8<sup>+</sup> T cells, we did not see a noteworthy expansion of γδ T cells under BLN treatment from PBMCs up to day 7. As expected there was no significant increase in T-cell counts in the absence of BLN (Figure 5, grey lines). Interestingly we saw higher expansion rates of both CD4<sup>+</sup> and CD8<sup>+</sup> T cells in the presence of high target cell density compared to other two conditions with medium and low target cell density at day 3. At day 7, there were no differences among these conditions in CD4<sup>+</sup> T cells. In CD8<sup>+</sup> T cells however, the cultures with the highest CD19<sup>+</sup> cells at baseline had the lowest CD8<sup>+</sup> T-cell counts at day 7 compared to the other two cultures

with medium and low frequencies of CD19<sup>+</sup> cells (red filled mark). This was confirmed by strongest activation profile (CD25<sup>+</sup>, HLA-DR<sup>+</sup>) in the presence of high target cells (not shown), compared to other cultures, where EM CD8<sup>+</sup> T cells predominated the BLN-containing cocultures on day 7, whereas the “naïve” population almost disappeared. In summary BLN application did not lead to γδ T-cell expansion in the presence of other T-cell populations, CD8<sup>+</sup> T cells were the most expanded subset, as previously reported (53) and target load was inversely correlated with absolute CD8<sup>+</sup> T-cell counts, suggestive of activation-associated contraction following strong activation.

## scRNA-seq reveals strong activation/exhaustion programs in $\alpha\beta$ T cells

To compare transcriptional profiles of  $\alpha\beta$  and  $\gamma\delta$  T cells following BLN stimulation at single-cell resolution, we performed targeted single-cell RNA sequencing of T cells from one healthy donor using the BD Rhapsody™ platform with a human T-cell panel focusing on key genes involved in T-cell responses. PBMCs from a healthy donor (containing autologous B cells) were cultured for 3 days with or without BLN (20 ng/ml). Subsequently, CD3<sup>+</sup> T cells were negatively isolated for sequencing. In parallel, immunophenotyping was performed using AbSeq reagents and conventional flow cytometry to support cluster identification and validate phenotypic states (Supplementary Figures 8A-D). After quality control and removing non-viable cells, 6872 high-quality T cells were included in the analysis. Dimensionality reduction and Seurat-based clustering on UMAP space identified 14 initial clusters (Supplementary Figure 8C), which were manually curated and consolidated into eight main functional clusters (groups) based on top 5 characteristic genes (Supplementary Table 4, Figure 6C,

Supplementary Figure 8). UMAP projection showed a clear separation between BLN-treated (red, 3, 576 cells) and untreated (grey 3, 296 cells) conditions, indicating major shifts in transcriptomic profiles upon BLN stimulation. UMAP projection shows minimal transcriptomic shifts in  $\gamma\delta$  T cells (predominantly Seurat clusters 6 and 13; Figures 6A, B, blue) following BLN exposure, with substantial overlap between -BLN and +BLN cells. In contrast,  $\alpha\beta$  T cells, especially CD8<sup>+</sup> T cells, redistributed into BLN-enriched regions and upregulated proliferation/effector and exhaustion-associated signatures (Figures 6B, C). BLN stimulation led to increased expression of genes associated with proliferation and effector function, as well as exhaustion markers including TIGIT, TIM-3 (HAVCR2), LAG3, and CD160 (Supplementary Figure 8B). In contrast,  $\gamma\delta$  T-cell frequencies remained largely stable, consistent with the phenotypic data and aligned with *in vitro*, with lack of  $\gamma\delta$  T cell expansion from PBMCs at day 3 as shown in Figure 5. Of note again, also on transcript level, exhaustion marker TIGIT was not expressed on  $\gamma\delta$  T cells following BLN exposure (Supplementary Figure 8B) (54).



## Discussion

BLN is a highly potent bispecific T-cell engager directing T-cell-mediated cytotoxicity toward CD19-expressing malignant blasts and normal B cells. In this study, we dissected BLN-mediated cytotoxic mechanisms by directly comparing resting and activated CD3-expressing conventional  $\alpha\beta$  T cells (CD4<sup>+</sup> and CD8<sup>+</sup>) and non-conventional  $\gamma\delta$  T cells, to evaluate their cytotoxic functions and phenotypic shifts following BLN stimulation.

Here we show that BLN efficiently redirected cytotoxicity toward CD19<sup>+</sup> targets across  $\alpha\beta$  and  $\gamma\delta$  T-cell subsets. However, freshly isolated  $\gamma\delta$  T cells demonstrated reduced BLN-mediated cytotoxicity against CD19<sup>+</sup> tumor cells compared to  $\alpha\beta$  T cells. Because BLN binds CD3 $\epsilon$  rather than the TCR variable domains, differences between  $\alpha\beta$  and  $\gamma\delta$  T cells under BLN likely reflect CD3 epitope/clone biology and CD3 glycosylation. In addition, lineage-specific signaling might also play a role, as antigen stimulation of the  $\gamma\delta$  TCR itself does not trigger CD3 conformational change (CD3 CC), in contrast to  $\alpha\beta$  T cells (29, 55–57). In human V $\gamma$ 9V $\delta$ 2  $\gamma\delta$  T cells, effects of anti-CD3 clones differ markedly: UCHT1 clone enforces CD3 CC and strongly augments  $\gamma\delta$  cytotoxicity, whereas OKT3 clone is comparatively weak unless valency is increased or CD3 is deglycosylated (55). In BLN CD3 scFv derives from murine L2K 07 clone. Some older reviews have mentioned TR66 as the parental clone of anti-CD3 for BLN (58), but more recent primary sources identify L2K-07 as the basis (59–61). However, direct functional comparison of clone L2K 07 with UCHT1 and OKT3 in  $\gamma\delta$  T cells are still missing.

Among  $\alpha\beta$  T cells, CD8<sup>+</sup> T cells mount a stronger response to BLN than CD4<sup>+</sup> T cells, consistent with prior reports showing superior cytotoxic potency of CD8<sup>+</sup> T cells in the presence of BLN (53). Collectively, these findings support notion that, *in vivo*, CD8<sup>+</sup> T cells are the principal contributors to therapeutic responses to BLN. Given the low  $\gamma\delta$  T-cell frequencies in blood, these cells are readily outcompeted by  $\alpha\beta$  cells in mixed cultures, which likely contributed to the minimal  $\gamma\delta$  expansion observed *ex vivo*.

In contrast,  $\gamma\delta$  T-cell lines, activated and expanded *ex vivo* using Zole, which selectively expands the V $\gamma$ 9V $\delta$ 2  $\gamma\delta$  T-cell subset, exhibited comparable cytotoxic efficacy to PHA-expanded  $\alpha\beta$  T cells. Across experiments, antigen density and tumor burden emerged as dominant modulators of potency, and BLN dosing further tuned  $\gamma\delta$  T-cell activity. Both Zole-expanded  $\gamma\delta$  and PHA-expanded  $\alpha\beta$  T cells cleared CD19<sup>+</sup> targets under low tumor burden (modelling MRD setting in ALL), whereas under high tumor burden (diagnosis/relapse-like)  $\alpha\beta$  T cells rapidly eliminated CD19<sup>+</sup> targets, and  $\gamma\delta$  T-cell killing improved with higher BLN concentration over time (29). Other T-cell engager designs most likely constructed with the same CD3–binder lineage as BLN (62) (e.g., HER2 $\times$ CD3) have shown potent  $\gamma\delta$ -mediated cytotoxicity *in vitro*. These experiments used much higher bispecific doses and higher effector-to-target ratios compared to conditions here (57, 62). These data do not suggest an intrinsic inability of  $\gamma\delta$  T cells to respond to CD3-engagers; rather, under the conditions tested, BLN elicited stronger responses in  $\alpha\beta$  than  $\gamma\delta$  T cells. They show potency of BLN-stimulated  $\gamma\delta$  T cells and that  $\alpha\beta$  cells respond more

robustly to BLN than  $\gamma\delta$  cells, at the cost of a higher risk of overt activation. We showed that BLN triggered sustained surface CD3 down-modulation in  $\alpha\beta$  T cells but not in  $\gamma\delta$  T cells, particularly at high target-load and was accompanied by consistently higher sFas-L release in  $\alpha\beta$  cultures. High disease burden amplifies BLN-driven synapse frequency and CD3 signaling (40), which might predispose  $\alpha\beta$  T cells to early AICD. This level of TCR-CD3 engagement is known to induce CD3 down modulation (internalization and  $\zeta$  chain degradation) and to trigger Fas/FasL mediated AICD on re-stimulation (45). Our observation of higher sFas-L secretion together with early CD3 down-modulation in  $\alpha\beta$  therefore is consistent with increased activation and suggests a greater susceptibility for Fas/FasL-associated apoptosis in  $\alpha\beta$  (particularly CD8<sup>+</sup>) T cells under high target load. However, AICD was not directly quantified in these experiments, and direct apoptosis measurements at early time points (e.g., Annexin V/active caspase-3) will be required to formally test this mechanism in future studies. Further, the preferential CD8 T-cell expansion at lower target load from co-cultures of activated T cells and mixed PBMC cultures supports this hypothesis. Clinically, the same principle underlies superior BLN outcomes at lower leukemia burden, the use of debulking, and BLN is frequently used in MRD settings and as a bridge to allogeneic transplantation (8, 12, 63, 64). This altogether suggests that high CD19 load accelerates  $\alpha\beta$  activation but limits CD8<sup>+</sup> expansion, whereas Zole-expanded V $\gamma$ 9V $\delta$ 2  $\gamma\delta$  T cells retain CD3 and maintain surface CD3 under these conditions; whether this reflects reduced susceptibility to AICD requires direct testing.

Importantly day 14 Zole-expanded  $\gamma\delta$  T cells displayed an effector phenotype with low expression of inhibitory checkpoints. Conversely, PHA-expanded  $\alpha\beta$  T cells underwent rapid activation and differentiation from naïve to EM. Single-cell RNA-seq from one donor supported these findings:  $\alpha\beta$  cells acquired proliferative and activation/exhaustion programs, whereas  $\gamma\delta$  cells showed comparatively modest transcriptional shifts. Larger sample sets are required to validate these findings.

In our assays,  $\gamma\delta$  cultures while exerting cytotoxic effector functions, produced lower IFN $\gamma$  and cytotoxic-granule release than  $\alpha\beta$  cultures and did not expand under BLN stimulation. Cytokine release syndrome (CRS) and Immune Effector Cell-Associated Neurotoxicity Syndrome (ICANS) are associated with systemic cytokine surges and widespread T-cell activation during CD3-engager therapy; However, our experiments were not designed to model these clinical toxicities, and cytokine levels and BLN exposure conditions *in vitro* may not reflect *in-vivo* exposure dynamics. Thus, these features may suggest a distinct inflammatory profile of  $\gamma\delta$ -based strategies. Whether  $\gamma\delta$  adoptive transfer alongside BLN therapy can deliver additional tumor control and how it impacts the incidence or severity of CRS/ICANS remains to be tested in future preclinical studies and clinical trials.

Zole expansion protocols have become a standard approach for generating clinical-grade  $\gamma\delta$  T-cell products (39). Several ongoing clinical trials (19) are evaluating Zole-expanded  $\gamma\delta$  T cells, both as monotherapy and in combination with BLN, to enhance treatment efficacy and improve T-cell fitness, especially in the context of heavily

pretreated patients undergoing chemotherapy. A key advantage of  $\gamma\delta$  T cells in adoptive transfer settings is their innate-like, non-alloreactive profile, eliminating concerns related to GvHD, thus making them particularly attractive for allogeneic and off-the-shelf therapy. Taken together with the target-burden dependence observed here, combining adoptive  $\gamma\delta$  T-cell transfer with BLN may be most plausibly explored in low-burden/MRD-like settings and/or in patients with impaired  $\alpha\beta$  T-cell fitness; this hypothesis requires dedicated preclinical testing and clinical evaluation, as supported by preclinical CD19-BiTE and V $\gamma$ 9V $\delta$ 2  $\gamma\delta$  T-cell synergy (34). Additionally, optimizing  $\gamma\delta$  T-cell expansion protocols, for instance, incorporating cytokines IL-2, IL-15, and vitamin C, has been shown to significantly boost cytotoxic function and proliferation while reducing apoptosis, suggesting a promising direction for future clinical applications. This approach with 414 expanded  $\gamma\delta$  T-cell infusions into 132 cancer patients has been shown to be clinically safe without significant adverse effects and prolonged the survival of late-stage cancer patients who received  $\geq 5$  cell infusions in a small cohort of 8 liver and 10 lung cancer patients (32).

In conclusion, our findings emphasize the therapeutic potential of  $\gamma\delta$  T cells in adoptive T-cell therapies, particularly when expanded *ex vivo* with Zole (19, 39, 44). Their stable cytotoxic functionality, maintenance of CD3 expression under BLN stimulation, together with lack of alloreactivity, may offer advantages for the design of adoptive immunotherapy protocols, pending validation in patient-derived models and clinical studies. Future clinical studies are warranted to evaluate the clinical efficacy and long-term benefits of Zole-expanded  $\gamma\delta$  T-cell products alone or in combination with BLN and other immune modulators, to harness their full therapeutic potential and improve outcomes for patients with CD19-expressing malignancies.

## Data availability statement

The original contributions presented in the study are included in the article/Supplementary Material. Further inquiries can be directed to the corresponding author.

## Ethics statement

The studies involving humans were approved by Institutional ethics review board of the University Medical Faculty Kiel (approval number D405/10, D479/18, D546/16). The studies were conducted in accordance with the local legislation and institutional requirements. The participants provided their written informed consent to participate in this study.

## Author contributions

MK: Data curation, Visualization, Methodology, Writing – original draft. NN: Writing – review & editing, Data curation,

Methodology. SB: Methodology, Data curation, Writing – review & editing, Validation. DK: Writing – review & editing, Formal analysis. ML: Writing – review & editing, Methodology. HT: Writing – review & editing. AL: Resources, Methodology, Writing – review & editing. CP: Resources, Writing – review & editing, Methodology. DW: Methodology, Writing – review & editing, Resources. H-HO: Methodology, Resources, Writing – review & editing. OJ: Writing – review & editing, Funding acquisition, Supervision. TV: Writing – review & editing, Supervision. CB: Writing – review & editing, Supervision. AS: Writing – review & editing, Funding acquisition, Resources. MB: Funding acquisition, Writing – review & editing, Resources, Supervision, Methodology. GC: Visualization, Conceptualization, Formal analysis, Funding acquisition, Methodology, Supervision, Writing – review & editing.

## Funding

The author(s) declared that financial support was received for this work and/or its publication. This study was supported by the Deutsche José Carreras Leukämie-Stiftung (DJCLS 22R/2019) to GC, MB, OJ and AS. This study was in part funded by the Deutsche Forschungsgemeinschaft (DFG, German Research Foundation) –project number 444949889 (KFO 5010 Clinical Research Unit ‘CATCH ALL’ to GC, SB, CB, MB, ML and TV), and through the “Clinician Scientist Program in Evolutionary Medicine” (Project number 413490537 to GC).

## Acknowledgments

We dedicate this work to the memory of Dr. Marcus Lettau, whose scientific insight, commitment, and collegial spirit were central to the conception of this study. Together with the corresponding author, he designed the project and initiated key experiments that formed the foundation of the present work. His enthusiasm for translational immunology and mentorship continues to inspire our research.

## Conflict of interest

The authors declared that this work was conducted in the absence of any commercial or financial relationships that could be construed as a potential conflict of interest.

## Generative AI statement

The authors declared that Generative AI was used in the creation of this manuscript. We used an AI language model (ChatGPT 5.2) solely for English-language editing during the revision process and did not use it for generating scientific content, data, dataanalyses, or conclusions.

Any alternative text (alt text) provided alongside figures in this article has been generated by Frontiers with the support of artificial intelligence and reasonable efforts have been made to ensure accuracy, including review by the authors wherever possible. If you identify any issues, please contact us.

## Publisher's note

All claims expressed in this article are solely those of the authors and do not necessarily represent those of their affiliated

organizations, or those of the publisher, the editors and the reviewers. Any product that may be evaluated in this article, or claim that may be made by its manufacturer, is not guaranteed or endorsed by the publisher.

## Supplementary material

The Supplementary Material for this article can be found online at: <https://www.frontiersin.org/articles/10.3389/fimmu.2026.1739493/full#supplementary-material>

## References

- Liu D, Zhao J, Song Y, Luo X, Yang T. Clinical trial update on bispecific antibodies, antibody-drug conjugates, and antibody-containing regimens for acute lymphoblastic leukemia. *J Hematol Oncol.* (2019) 12:15. doi: 10.1186/s13045-019-0703-z
- Chitadze G, Laqua A, Lettau M, Baldus CD, Bruggemann M. Bispecific antibodies in acute lymphoblastic leukemia therapy. *Expert Rev Hematol.* (2020) 13:1211–33. doi: 10.1080/17474086.2020.1831380
- Dinmohamed AG, Szabo A, van der Mark M, Visser O, Sonneveld P, Cornelissen JJ, et al. Improved survival in adult patients with acute lymphoblastic leukemia in the Netherlands: a population-based study on treatment, trial participation and survival. *Leukemia.* (2016) 30:310–7. doi: 10.1038/leu.2015.230
- Fredman D, Moshe Y, Wolach O, Heering G, Shichrur K, Goldberg I, et al. Evaluating outcomes of adult patients with acute lymphoblastic leukemia and lymphoblastic lymphoma treated on the GMALL 07/2003 protocol. *Ann Hematol.* (2022) 101:581–93. doi: 10.1007/s00277-021-04738-y
- Möricke A, Zimmermann M, Valsecchi MG, Stanulla M, Biondi A, Mann G, et al. Dexamethasone vs prednisone in induction treatment of pediatric ALL: results of the randomized trial AIEOP-BFM ALL 2000. *Blood.* (2016) 127:2101–12. doi: 10.1182/blood-2015-09-670729
- Baden D, Wolgast N, Altröck PM, Steinhäuser S, Voran J, Beder T, et al. Epidemiology, survival, and treatment of acute myeloid and lymphoblastic leukaemia in Germany: a nationwide population-based registry analysis. *Lancet Regional Health - Europe.* (2025) 59:101503. doi: 10.1016/j.lanep.2025.101503
- Bargou R, Leo E, Zugmaier G, Klinger M, Goebeler M, Knop S, et al. Tumor regression in cancer patients by very low doses of a T cell-engaging antibody. *Science.* (2008) 321:974–7. doi: 10.1126/science.1158545
- Kantarjian H, Stein A, Gokbuget N, Fielding AK, Schuh AC, Ribera JM, et al. Blinatumomab versus chemotherapy for advanced acute lymphoblastic leukemia. *N Engl J Med.* (2017) 376:836–47. doi: 10.1056/NEJMoa1609783
- von Stackelberg A, Locatelli F, Zugmaier G, Handgretinger R, Trippett TM, Rizzari C, et al. Phase I/phase II study of blinatumomab in pediatric patients with relapsed/refractory acute lymphoblastic leukemia. *J Clin Oncol.* (2016) 34:4381–9. doi: 10.1200/JCO.2016.67.3301
- Gupta S, Rau RE, Kairalla JA, Rabin KR, Wang C, Angiolillo AL, et al. Blinatumomab in standard-risk B-cell acute lymphoblastic leukemia in children. *N Engl J Med.* (2025) 392:875–91. doi: 10.1056/NEJMoa2411680
- Litzow MR, Sun Z, Mattison RJ, Paietta EM, Roberts KG, Zhang Y, et al. Blinatumomab for MRD-negative acute lymphoblastic leukemia in adults. *N Engl J Med.* (2024) 391:320–33. doi: 10.1056/NEJMoa2312948
- Gokbuget N, Dombret H, Bonifacio M, Reichle A, Graux C, Faul C, et al. Blinatumomab for minimal residual disease in adults with B-cell precursor acute lymphoblastic leukemia. *Blood.* (2018) 131:1522–31. doi: 10.1182/blood-2017-08-798322
- Topp MS, Gokbuget N, Stein AS, Zugmaier G, O'Brien S, Bargou RC, et al. Safety and activity of blinatumomab for adult patients with relapsed or refractory B-precursor acute lymphoblastic leukaemia: a multicentre, single-arm, phase 2 study. *Lancet Oncol.* (2015) 16:57–66. doi: 10.1016/S1470-2045(14)71170-2
- Locatelli F, Shah B, Thomas T, Velasco K, Adedokun B, Aldoss I, et al. Incidence of CD19-negative relapse after CD19-targeted immunotherapy in R/R BCP acute lymphoblastic leukemia: a review. *Leuk Lymphoma.* (2023) 64:1615–33. doi: 10.1080/10428194.2023.2232496
- Das RK, O'Connor RS, Grupp SA, Barrett DM. Lingering effects of chemotherapy on mature T cells impair proliferation. *Blood Adv.* (2020) 4:4653–64. doi: 10.1182/bloodadvances.2020001797
- Philipp N, Kazerani M, Nicholls A, Vick B, Wulf J, Straub T, et al. T-cell exhaustion induced by continuous bispecific molecule exposure is ameliorated by treatment-free intervals. *Blood.* (2022) 140:1104–18. doi: 10.1182/blood.2022015956
- Hijazi Y, Klinger M, Kratzer A, Wu B, Baeuerle PA, Kufer P, et al. Pharmacokinetic and pharmacodynamic relationship of blinatumomab in patients with non-hodgkin lymphoma. *Curr Clin Pharmacol.* (2018) 13:55–64. doi: 10.2174/1574884713666180518102514
- Kabelitz D, Serrano R, Kouakanou L, Peters C, Kalyan S. Cancer immunotherapy with gammadelta T cells: many paths ahead of us. *Cell Mol Immunol.* (2020) 17:925–39. doi: 10.1038/s41423-020-0504-x
- Hayday A, Dechanet-Merville J, Rossjohn J, Silva-Santos B. Cancer immunotherapy by gammadelta T cells. *Science.* (2024) 386:eabq7248. doi: 10.1126/science.abq7248
- Gober HJ, Kistowska M, Angman L, Jenö P, Mori L, De Libero G. Human T cell receptor gammadelta cells recognize endogenous mevalonate metabolites in tumor cells. *J Exp Med.* (2003) 197:163–8. doi: 10.1084/jem.20021500
- Willcox CR, Mohammed F, Willcox BE. The distinct MHC-unrestricted immunobiology of innate-like and adaptive-like human gammadelta T cell subsets-Nature's CAR-T cells. *Immunol Rev.* (2020) 298:25–46. doi: 10.1111/imr.12928
- Gaballa A, Arruda LCM, Uhlin M. Gamma delta T-cell reconstitution after allogeneic HCT: A platform for cell therapy. *Front Immunol.* (2022) 13:971709. doi: 10.3389/fimmu.2022.971709
- Godder KT, Henslee-Downey PJ, Mehta J, Park BS, Chiang KY, Abhyankar S, et al. Long term disease-free survival in acute leukemia patients recovering with increased gammadelta T cells after partially mismatched related donor bone marrow transplantation. *Bone Marrow Transplant.* (2007) 39:751–7. doi: 10.1038/sj.bmt.1705650
- Esin S, Shigematsu M, Nagai S, Eklund A, Wigzell H, Grunewald J. Different percentages of peripheral blood gamma delta + T cells in healthy individuals from different areas of the world. *Scand J Immunol.* (1996) 43:593–6. doi: 10.1046/j.1365-3083.1996.d01-79.x
- Davey MS, Willcox CR, Hunter S, Kasatskaya SA, Remmerswaal EBM, Salim M, et al. The human Vdelta2(+) T-cell compartment comprises distinct innate-like Vgamma9(+) and adaptive Vgamma9(-) subsets. *Nat Commun.* (2018) 9:1760. doi: 10.1038/s41467-018-04076-0
- Roelofs AJ, Jauhainen M, Monkkonen H, Rogers MJ, Monkkonen J, Thompson K. Peripheral blood monocytes are responsible for gammadelta T cell activation induced by zoledronic acid through accumulation of IPP/DMAAPP. *Br J Haematol.* (2009) 144:245–50. doi: 10.1111/j.1365-2141.2008.07435.x
- Kondo M, Sakuta K, Noguchi A, Ariyoshi N, Sato K, Sato S, et al. Zoledronate facilitates large-scale ex vivo expansion of functional gammadelta T cells from cancer patients for use in adoptive immunotherapy. *Cytotherapy.* (2008) 10:842–56. doi: 10.1080/14653240802419328
- Harly C, Guillaume Y, Nedellec S, Peigne CM, Monkkonen H, Monkkonen J, et al. Key implication of CD277/butyrophilin-3 (BTN3A) in cellular stress sensing by a major human gammadelta T-cell subset. *Blood.* (2012) 120:2269–79. doi: 10.1182/blood-2012-05-430470
- Rigau M, Ostrowska S, Fulford TS, Johnson DN, Woods K, Ruan Z, et al. Butyrophilin 2A1 is essential for phosphoantigen reactivity by  $\gamma\delta$  T cells. *Science.* (2020) 367:eaay5516. doi: 10.1126/science.aay5516
- Brandes M, Willmann K, Boley G, Levy N, Eberl M, Luo M, et al. Cross-presenting human gammadelta T cells induce robust CD8+ alphabeta T cell responses. *Proc Natl Acad Sci U.S.A.* (2009) 106:2307–12. doi: 10.1073/pnas.0810059106
- Holmen Olofsson G, Idorn M, Carnaz Simoes AM, Aehnlich P, Skadborg SK, Noessner E, et al. Vgamma9Vdelta2 T cells concurrently kill cancer cells and cross-present tumor antigens. *Front Immunol.* (2021) 12:645131. doi: 10.3389/fimmu.2021.645131

32. Xu Y, Xiang Z, Alnaggar M, Kouakanou L, Li J, He J, et al. Allogeneic Vgamma9Vdelta2 T-cell immunotherapy exhibits promising clinical safety and prolongs the survival of patients with late-stage lung or liver cancer. *Cell Mol Immunol.* (2021) 18:427–39. doi: 10.1038/s41423-020-0515-7
33. Kelm M, Darzentas F, Darzentas N, Kotrova M, Wessels W, Bendig S, et al. Dominant T-cell receptor delta rearrangements in B-cell precursor acute lymphoblastic leukemia: leukemic markers or physiological gammadelta T repertoire? *Hemasphere.* (2023) 7:e948. doi: 10.1097/HS9.0000000000000948
34. Chen YH, Wang Y, Liao CH, Hsu SC. The potential of adoptive transfer of gamma9delta2 T cells to enhance blinatumomab's antitumor activity against B-cell Malignancy. *Sci Rep.* (2021) 11:12398. doi: 10.1038/s41598-021-91784-1
35. You H, Zhu H, Zhao Y, Guo J, Gao Q. TIGIT-expressing zoledronate-specific gammadelta T cells display enhanced antitumor activity. *J Leukoc Biol.* (2022) 112:1691–700. doi: 10.1002/JLB.5MA0822-759R
36. Chen D, Guo Y, Jiang J, Wu P, Zhang T, Wei Q, et al. gammadelta T cell exhaustion: Opportunities for intervention. *J Leukoc Biol.* (2022) 112:1669–76. doi: 10.1002/JLB.5MR0722-777R
37. Bender A, Kabelitz D. CD4-CD8- human T cells: phenotypic heterogeneity and activation requirements of freshly isolated "double-negative" T cells. *Cell Immunol.* (1990) 128:542–54. doi: 10.1016/0008-8749(90)90047-u
38. Katzen D, Chu E, Terhost C, Leung DY, Gesner M, Miller RA, et al. Mechanisms of human T cell response to mitogens: IL 2 induces IL 2 receptor expression and proliferation but not IL 2 synthesis in PHA-stimulated T cells. *J Immunol.* (1985) 135:1840–5. doi: 10.4049/jimmunol.135.3.1840
39. Peters C, Kouakanou L, Oberg HH, Wesch D, Kabelitz D. *In vitro* expansion of Vgamma9Vdelta2 T cells for immunotherapy. *Methods Enzymol.* (2020) 631:223–37. doi: 10.1016/bs.mie.2019.07.019
40. Liu C, Zhou J, Kudlacek S, Qi T, Dunlap T, Cao Y. Population dynamics of immunological synapse formation induced by bispecific T cell engagers predict clinical pharmacodynamics and treatment resistance. *Elife.* (2023) 12. doi: 10.7554/eLife.83659
41. Hao Y, Stuart T, Kowalski MH, Choudhary S, Hoffman P, Hartman A, et al. Dictionary learning for integrative, multimodal and scalable single-cell analysis. *Nat Biotechnol.* (2024) 42:293–304. doi: 10.1038/s41587-023-01767-y
42. Saini RV, Wilson C, Finn MW, Wang T, Krensky AM, Clayberger C. Granulysin delivered by cytotoxic cells damages endoplasmic reticulum and activates caspase-7 in target cells. *J Immunol.* (2011) 186:3497–504. doi: 10.4049/jimmunol.1003409
43. Seder RA, Ahmed R. Similarities and differences in CD4+ and CD8+ effector and memory T cell generation. *Nat Immunol.* (2003) 4:835–42. doi: 10.1038/ni969
44. Kondo M, Izumi T, Fujieda N, Kondo A, Morishita T, Matsushita H, et al. Expansion of human peripheral blood gammadelta T cells using zoledronate. *J Vis Exp.* (2011) (55):3182. doi: 10.3791/3182
45. Green DR, Droin N, Pinkoski M. Activation-induced cell death in T cells. *Immunol Rev.* (2003) 193:70–81. doi: 10.1034/j.1600-065x.2003.00051.x
46. Ebsen H, Lettau M, Kabelitz D, Janssen O. Subcellular localization and activation of ADAM proteases in the context of FasL shedding in T lymphocytes. *Mol Immunol.* (2015) 65:416–28. doi: 10.1016/j.molimm.2015.02.008
47. Dreier T, Lorenczewski G, Brandl C, Hoffmann P, Syring U, Hanakam F, et al. Extremely potent, rapid and costimulation-independent cytotoxic T-cell response against lymphoma cells catalyzed by a single-chain bispecific antibody. *Int J Cancer.* (2002) 100:690–7. doi: 10.1002/ijc.10557
48. Baeuerle PA, Kufer P, Bargou R. BiTE: Teaching antibodies to engage T-cells for cancer therapy. *Curr Opin Mol Ther.* (2009) 11:22–30.
49. Hoffmann P, Hofmeister R, Brischwein K, Brandl C, Crommer S, Bargou R, et al. Serial killing of tumor cells by cytotoxic T cells redirected with a CD19-/CD3-bispecific single-chain antibody construct. *Int J Cancer.* (2005) 115:98–104. doi: 10.1002/ijc.20908
50. Zhu M, Kratzer A, Johnson J, Holland C, Brandl C, Singh I, et al. Blinatumomab pharmacodynamics and exposure-response relationships in relapsed/refractory acute lymphoblastic leukemia. *J Clin Pharmacol.* (2018) 58:168–79. doi: 10.1002/jcph.1006
51. Valitutti S, Muller S, Salio M, Lanzavecchia A. Degradation of T cell receptor (TCR)-CD3-zeta complexes after antigenic stimulation. *J Exp Med.* (1997) 185:1859–64. doi: 10.1084/jem.185.10.1859
52. Suda T, Hashimoto H, Tanaka M, Ochi T, Nagata S. Membrane Fas ligand kills human peripheral blood T lymphocytes, and soluble Fas ligand blocks the killing. *J Exp Med.* (1997) 186:2045–50. doi: 10.1084/jem.186.12.2045
53. Klinger M, Brandl C, Zugmaier G, Hijazi Y, Bargou RC, Topp MS, et al. Immunopharmacologic response of patients with B-lineage acute lymphoblastic leukemia to continuous infusion of T cell-engaging CD19/CD3-bispecific BiTE antibody blinatumomab. *Blood.* (2012) 119:6226–33. doi: 10.1182/blood-2012-01-400515
54. Rancan C, Arias-Badia M, Dogra P, Chen B, Aran D, Yang H, et al. Exhausted intratumoral Vdelta2(-) gammadelta T cells in human kidney cancer retain effector function. *Nat Immunol.* (2023) 24:612–24. doi: 10.1038/s41590-023-01448-7
55. Dopfer EP, Hartl FA, Oberg HH, Siegers GM, Yousefi OS, Kock S, et al. The CD3 conformational change in the gammadelta T cell receptor is not triggered by antigens but can be enforced to enhance tumor killing. *Cell Rep.* (2014) 7:1704–15. doi: 10.1016/j.celrep.2014.04.049
56. Oberg HH, Kellner C, Gonnermann D, Peipp M, Peters C, Sebens S, et al. gammadelta T cell activation by bispecific antibodies. *Cell Immunol.* (2015) 296:41–9. doi: 10.1016/j.cellimm.2015.04.009
57. Alarcon B, De Vries J, Pettey C, Boylston A, Yssel H, Terhorst C, et al. The T-cell receptor gamma chain-CD3 complex: implication in the cytotoxic activity of a CD3+ CD4- CD8- human natural killer clone. *Proc Natl Acad Sci U.S.A.* (1987) 84:3861–5. doi: 10.1073/pnas.84.11.3861
58. Burt R, Warcel D, Fielding AK. Blinatumomab, a bispecific B-cell and T-cell engaging antibody, in the treatment of B-cell Malignancies. *Hum Vaccin Immunother.* (2019) 15:594–602. doi: 10.1080/21645515.2018.1540828
59. Jacobs N, Mazzoni A, Mezzanzanica D, Negri DR, Valota O, Colnaghi MI, et al. Efficiency of T cell triggering by anti-CD3 monoclonal antibodies (mAb) with potential usefulness in bispecific mAb generation. *Cancer Immunol Immunother.* (1997) 44:257–64. doi: 10.1007/s002620050381
60. Mocquot P, Mossazadeh Y, Lapierre L, Pineau F, Despas F. The pharmacology of blinatumomab: state of the art on pharmacodynamics, pharmacokinetics, adverse drug reactions and evaluation in clinical trials. *J Clin Pharm Ther.* (2022) 47:1337–51. doi: 10.1111/jcpt.13741
61. *Blinatumomab (AMG 103, BLINCYTO®)* (2025). Available online at: <https://dctd.cancer.gov> (Accessed April 11, 2025).
62. Oberg HH, Peipp M, Kellner C, Sebens S, Krause S, Petrick D, et al. Novel bispecific antibodies increase gammadelta T-cell cytotoxicity against pancreatic cancer cells. *Cancer Res.* (2014) 74:1349–60. doi: 10.1158/0008-5472.CAN-13-0675
63. Queudeville M, Stein AS, Locatelli F, Ebinger M, Handgretinger R, Gokbuget N, et al. Low leukemia burden improves blinatumomab efficacy in patients with relapsed/refractory B-cell acute lymphoblastic leukemia. *Cancer.* (2023) 129:1384–93. doi: 10.1002/cncr.34667
64. Bonifacio M, Papayannidis C, Lussana F, Fracchiolla N, Annunziata M, Sica S, et al. Real-world multicenter experience in tumor debulking prior to blinatumomab administration in adult patients with relapsed/refractory B-cell precursor acute lymphoblastic leukemia. *Front Oncol.* (2021) 11:804714. doi: 10.3389/fonc.2021.804714